Article

Emergence of classical objectivity of quantum Darwinism in a photonic quantum simulator

Ming-Cheng Chen [a,b], Han-Sen Zhong [a,b], Yuan Li [a,b], Dian Wu [a,b], Xi-Lin Wang [a,b], Li Li [a,b], Nai-Le Liu [a,b], Chao-Yang Lu [a,b,*], Jian-Wei Pan [a,b]

[a] Hefei National Laboratory for Physical Sciences at Microscale and Department of Modern Physics, University of Science and Technology of China, Hefei 230026, China
[b] CAS Centre for Excellence and Synergetic Innovation Centre in Quantum Information and Quantum Physics, University of Science and Technology of China, Hefei 230026, China

ARTICLE INFO

ABSTRACT

Quantum-to-classical transition is a fundamental open question in physics frontier. Quantum decoherence theory points out that the inevitable interaction with environment is a sink carrying away quantum coherence, which is responsible for the suppression of quantum superposition in open quantum system. Recently, quantum Darwinism theory further extends the role of environment, serving as communication channel, to explain the classical objectivity emerging in quantum measurement process. Here, we used a six-photon quantum simulator to investigate classical and quantum information proliferation in quantum Darwinism process. In the simulation, many environmental photons are scattered from an observed quantum system and they are collected and used to infer the system's state. We observed redundancy of system's classical information and suppression of quantum correlation in the fragments of environmental photons. Our results experimentally show that the classical objectivity of quantum system can be established through quantum Darwinism mechanism.

© 2019 Science China Press. Published by Elsevier B.V. and Science China Press. All rights reserved.

1. Introduction

Quantum mechanics is a spectacularly successful predictive theory, but there is still an unresolved problem about its interpretation in quantum measurement problem [1]. The orthodox Copenhagen interpretation separates the world into quantum domain and classical domain, which is bridged by observation-induced collapse [2]. How the wave function collapses and classical objectivity emerges from a quantum substrate? A detailed mechanism of this quantum-to-classical transition is of fundamentally importance for developing a unified view of our physical world.

Quantum decoherence theory identifies that the uncontrolled interactions with the environment can destroy the coherence of a quantum system into a mixed state. In the theory, the environment is traced out and thus the system's classical behavior is explained in the level of ensemble average [3,4]. How the quantum system's classical objectivity arises in a single measurement event is still unresolved. Classical objectivity is a property that many observers can independently observe and establish a consensus view of the state of a quantum system without perturbing it [5]. In a general observation process, observers do not directly touch and interact with the quantum system. They perceive the system by collecting information from its surrounding environment.

Recently, quantum Darwinism explains the emergence of classical objectivity of a single quantum system through classical information broadcasting and proliferating in its environment [5,6]. The key idea is that the environment acts as communication channel and only classical information about the system can reach observers. The environment selects system's classical information to broadcast and proliferate, and observers use the redundant classical information in local environment fragments to perceive the state of system. In this process, many observers can independently and simultaneously query separate fragments of the environment and reach a consensus about the system's classical state. Specifically, the quantum Darwinism theory singles out a branch structure of system-environment (observers) composite quantum states [7–9] from measurement-like interaction to explain the appearance of classical pointer states. The classical pointer states are the eigenstates of the measurement observable.

In this work, we report a test of quantum Darwinism principle on a photonic quantum simulator [10,11] in view of information theory. We measured the information correlations between system and environment, where the system is a single photon and the environment is another five photons. Quantum mutual information, Holevo bound, and quantum discord [12–15] are used to

* Corresponding author.
E-mail address: cylu@ustc.edu.cn (C.-Y. Lu).

account for the total correlation, classical correlation, and pure quantum correlation, respectively. We used these correlations to investigate information broadcasting and proliferating.

2. Theory

The basic process of quantum Darwinism is shown in Fig. 1a. A central quantum system (single photon) is monitored by particles (photons) in the environment [16,17]. The particles are scattered from the system and caught by observers. These environment particles serve as individual memory cells which are imprinted of system's pointer-state information. When there are random interactions among the environment's particles, the stored information will be inevitably scrambled out. Hence, only non-interaction environment is good memory for redundant records of system's state.

We design a quantum Darwinism simulator shown in Fig. 1b to simulate non-interaction environment, such as daily photonic environment. In the simulator, a central qubit interacts with the environment qubits through two-qubit controlled-rotation gates $U(\theta) = |0\rangle\langle 0| \otimes I + |1\rangle\langle 1| \otimes R_y(\theta)$ with random angles to mimic the random scattering process, where $R_y(\theta)$ rotates a qubit by angle θ along the y axis of Bloch sphere. When the system qubit is initialized in superposition state $\alpha|0\rangle_S + \beta|1\rangle_S$, the simulator will produce Darwinist states with branch structure

$$\alpha|0\rangle_S \otimes_{i=1}^N |0\rangle_i + \beta|1\rangle_S \otimes_{i=1}^N \left(\cos\frac{\theta_i}{2}|0\rangle_i + \sin\frac{\theta_i}{2}|1\rangle_i \right), \quad (1)$$

where $|\alpha|^2 + |\beta|^2 = 1$ and N is the number of environment qubits.

The interaction with environment selects preferred pointer states of the observed system, which are the states left unchanged under the interactions and thus multiple records of the state can be faithfully copied into environment. For interactions generated from a Hamiltonian form of $H_i = g_i A \otimes B_i$, the eigenstates of monitored observable A are the pointer states, where A and B_i are two observables on system and environment particle i, respectively [5]. In our simulator setting, $A = (\sigma_I - \sigma_Z)/2, B_i = \sigma_X$ and $g_i \Delta t = \theta_i/2$, therefore, the pointer states from interaction $U(\theta_i) = e^{-iH_i\Delta t}$ are $|0\rangle$ and $|1\rangle$, respectively.

The pointer states can be quantified by the disappearance of quantum coherence

$$C(\rho_S) = H_{cl}(\rho_S) - H(\rho_S), \quad (2)$$

where ρ_S is the reduced density matrix of system, $H(\rho_S) = -\text{tr}(\rho_S \log_2 \rho_S)$ is quantum von-Neumann entropy and $H_{cl}(\rho_S) = -\text{tr}(\mathbf{p}_S \log_2 \mathbf{p}_S)$ is classical Shannon entropy, $\mathbf{p}_S$ is the diagonal elements of density matrix ρ_S in pointer-state bases [18,19]. The reality of pointer states will emerge when the quantum system is completely decohered by the environment. In this case, the classical entropy will equal to the quantum entropy. The efficiency of decoherence depends on the initial states of environment [17,20]. Impure or misaligned (close to the eigenstate of observable B_i) environment will reduce the decoherence efficiency. In our simulation, $|0\rangle$ states are used as initial environment states with optimal efficiency.

In quantum Darwinism process, the information about the quantum system is broadcast to the environment. Local observers can only access small fragments of the whole environment. The quantum mutual information

$$I(S : E_i) = H(\rho_S) + H\left(\rho_{E_i}\right) - H\left(\rho_{SE_i}\right), \quad (3)$$

can be used to quantify how much information an observer E_i (accessing the environment fragment E_i) knows about the quantum system [5]. When $I(S : E_i) \approx H(\rho_S)$ for all observers $\{E_i\}$, the system's state can be determined by all the observers and thus the quantum system becomes objective.

3. Experiment

We use a photonic simulator [10,11] (shown in Fig. 2) to produce quantum Darwinism states consisted of a central system qubit (photon 1) and five environment qubits (photons 2–6). The quantum state of system is observed at the superposition state $(|0\rangle + |1\rangle)/\sqrt{2}$. Two sets of rotation-angle parameter, $\vec{\theta}_A = (180°, 180°, 180°, 180°, 180°)$ and $\vec{\theta}_B = (180°, 180°, 180°, 72°, 100°)$, are used in the experiments from the following considerations. Note that here the phases in $\vec{\theta}_B$ are chosen merely to represent nonorthogonal case to simulate the small environment fragment without specific optimization.

A real environment fragment can contain many elementary subsystems. If the fragment is large, its quantum states can be simplified and expressed as orthogonal logical states $|0_L\rangle = \otimes_{i=1}^n |0\rangle_i$ and $|1_L\rangle = \otimes_{i=1}^n (\cos\frac{\theta_i}{2}|0\rangle_i + \sin\frac{\theta_i}{2}|1\rangle_i)$, due to $\langle 0_L|1_L\rangle = \prod_{i=1}^n \cos\frac{\theta_i}{2} \to 0$ for sufficiently large number n of subsystems in a fragment. Furthermore, if the fragment is small, its quantum states can be expressed as nonorthogonal logical states $|0_L\rangle$ and $\cos\frac{\theta}{2}|0_L\rangle + \sin\frac{\theta}{2}|1_L\rangle$. In our simulation, the photonic qubits represent the quantum state of environment fragments logically and an observer can access one or more fragments to infer the system's state. The parameter $\vec{\theta}_A$ is used to simulate 5 large environment fragments and parameter $\vec{\theta}_B$ is used to simulate 3 large environment fragments and 2 small environment fragments.

The experimental setup is shown in Fig. 2. The qubits are encoded in the horizontal (H) and vertical (V) polarization of single photons, which are produced by spontaneous parametric
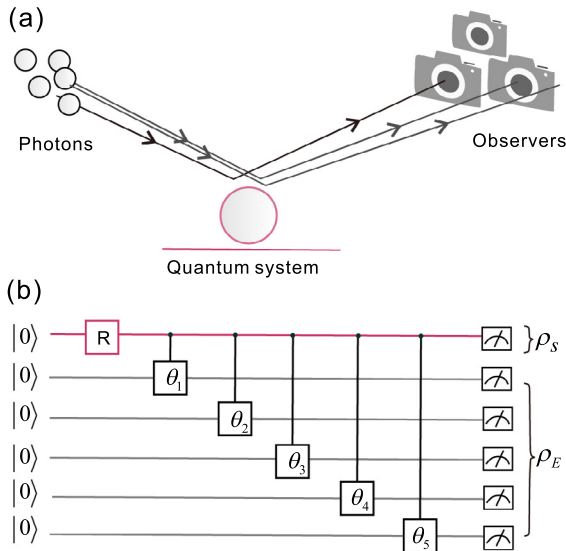

Fig. 1. (Color online) Quantum Darwinism process. (a) Multiple observers use independent fragments of the scattered environment photons to reveal the state of observed quantum system. They can determine the pointer states of the observed quantum system without perturbing it and thus agree on the observed outcome. As a result, the quantum system becomes classical and objective in this process. (b) A quantum simulator to simulate the system-environment interaction and produce quantum Darwinism states. In the simulator, the fist qubit is quantum system and the environment particles (other qubits) interact with the system of arbitrary interaction strengths $\{\theta_i\}$ in parallel and have no interaction between themselves. Measurements are performed on these particles to infer the information of quantum system.
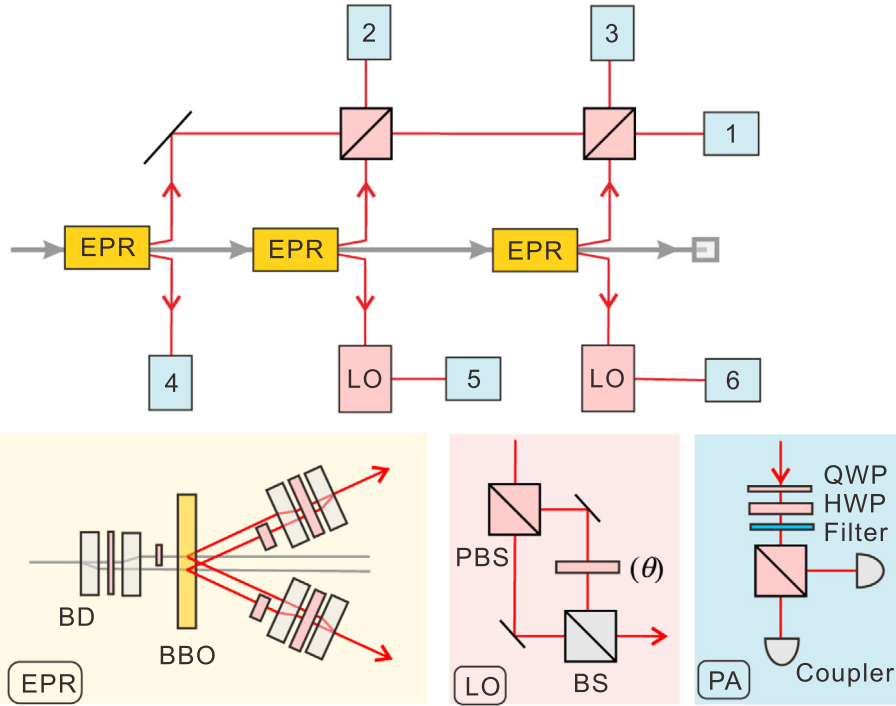
Fig. 2. (Color online) Experimental setup. A six-photon interferometer is used to produce the system-environment composite quantum Darwinism states. Photon 1 is the central quantum system and photons 2 − 6 are the environment. Infrared laser pulses (775 nm wavelength, 120 fs pulse duration, 80 MHz repetition rate) pass through three beta-barium borate (BBO) nonlinear crystals sequentially to produce three pairs of Einstein-Podolsky-Rosen(EPR) polarization-entangled photons. The two components of EPR state are independently produced and coherently combined by beam displacers (BDs). Three single photons, one from each pair (photons 1, 2 and 3), interfere on two polarization beam splitters (PBSs) to generate an entangled six photons in Greenberger-Horne-Zeilinger (GHZ) state. Two single photons (5 and 6) pass through polarization-dependent Mach-Zehnder (MZ) interferometers to realize local non-unitary operations (LOs). In the MZ interferometers, two polarization components of input photons are separated by polarization beam splitters and recombined on balanced beam splitters (BSs). The internal half-wave plates (HWP) are set at angle $\theta_5/4$ and $\theta_6/4$, respectively. All the photons are sent to polarization analysis (PA) setups, each consisting of a quarter-wave plate (QWP), a HWP, a spectrum filter, and a PBS. The photons are finally detected by fiber-coupled single-photon detectors and six-fold coincidence counting are registered. Note that our experimental setup is not a faithful simulator of the scattering process. Instead, we mainly want to simulate the process where scattered photons are used to infer the state of quantum system.

down-conversion (SPDC) process [21,22]. The Darwinism states in Eq. (1) are synthesized in three steps.

(1) Preparation of three pairs of polarization-entangled photons in Einstein-Polodsky-Rosen (EPR) state $(|HH\rangle + |VV\rangle)/\sqrt{2}$ [23] from SPDC process. With a laser pump power of 0.9 W, the generation probability of two twin photons is 0.025 and the fidelity of EPR state is above 99%.

(2) Three EPR pairs are combined on two polarization beam splitters, postselecting the entangled subspace of $|HH\rangle\langle HH| + |VV\rangle\langle VV|$, to produce a six-photon Greenberger-Horne-Zeilinger (GHZ) state $(|HHHHHH\rangle + |VVVVVV\rangle)/\sqrt{2}$ [24]. The success probability is 0.25.

(3) Two photons from the GHZ state are further operated by polarization-dependent Mach-Zehnder (MZ) interferometer. In the interferometer, the H and V components are separated by polarization beam splitters and then recombined on balanced beam splitters to implement non-unitary process $|H\rangle\langle H| + (\cos\frac{\theta}{2}|H\rangle + \sin\frac{\theta}{2}|V\rangle)\langle V|$ with a success probability 0.5.

The experiment runs with repetition rate 80 MHz and the single photons are measured with collecting and detecting efficiency of 0.65. Thus, we obtain six-photon coincidence counting rates about 5 counts/second. The quantum states are measured through quantum state tomography. There are 729 measurement settings and about 700 counts in each setting. Fig. 3a and b show the measured density matrices. For setting $\vec{\theta}_A$, the quantum state fidelity is

0.859 ± 0.002 and the purity is 0.777 ± 0.004. For setting $\vec{\theta}_B$, the quantum state fidelity is 0.703 ± 0.004 and the purity is 0.692 ± 0.006. The standard deviation is estimated from Monte Carlo method with 100 trials.

The quantum coherence $C(\rho_S)$ of system qubit in Eq. (2) are 0.001(4) and 0.020(6) in process $\vec{\theta}_A$ and $\vec{\theta}_B$, respectively, which indicates that the environment has fully decohered the system. The quantum mutual information $I(S : E_i)$, the Eq. (3), between the system and 31 different combinations of environment fragments are shown in the Fig. 3c and d, respectively. The results have two significant features. The mutual information quickly approaches the system's entropy $H(\rho_S)$ (exceeding 70%, mainly limited by the purity of prepared entangled quantum states) when accessing small environment fragments, and the mutual information is saturated when increasing the size of environment fragments.

The arrows in Fig. 3d show that the environment fragments 5 and 6 are two low-fidelity records of the system's states, which is expected from the corresponding nonorthogonal rotating angles in process $\vec{\theta}_B$. On the other hand, environment fragments 2346 and 2345 have mutual information exceeding the system's entropy. This indicates that the mutual information contains more information than system's information alone. We further analyze the information compositions by dividing it into the locally-accessible classical information and the extra information from pure quantum correlations. We show the classical correlation and quantum correlation between system and environment fragments in Fig. 4.
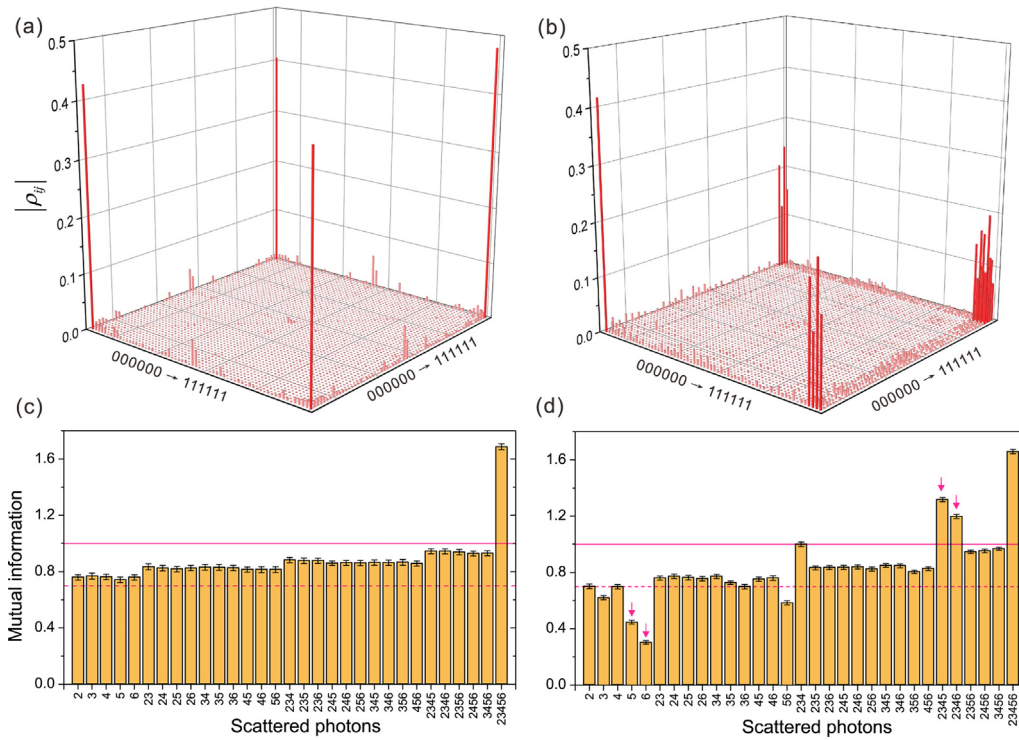
Fig. 3. (Color online) Experimental results. (a), (b) The absolute value of restructured density matrix elements of Darwinism states for parameter $\vec{\theta}_A$ and $\vec{\theta}_B$, respectively. The states are estimated by quantum state tomography with 729 measure settings. (c), (d) The mutual information between the system and the 31 different pieces of environment fragments for parameter $\vec{\theta}_A$ and $\vec{\theta}_B$, respectively. The red line indicates the classical entropy of system and the dotted line marks 70% of the classical entropy to guide the eye. The short arrows label four special environment fragments for further analysis in the main text.

The first one, Hovelo bound $\chi(S : E_i)$, measures the capacity of environment acting as communication channel to deliver system's classical information. The Hovelo bound

$$\chi(S : E_i) = \max_{\{M_s\}} \left\{ H\left(\sum_s p_s \rho_{E_i|s} \right) - \sum_s p_s H\left(\rho_{E_i|s} \right) \right\}, \quad (4)$$

is maximum mutual information of the classical-quantum state between system and environment fragments with optimal measurement $\{M_s\}$ on the system [14], where $\rho_{E_i|s}$ is quantum state of environment E_i conditioned on a measured result s on the system with probability p_s. The second one, quantum discord

$$D(S : E_i) = I(S : E_i) - \chi(S : E_i), \quad (5)$$

measures the loss of information due to the observers can only locally access the environment, which quantifies the pure quantum correlation between environment and system [14].

In Fig. 4, the classical correlations and quantum correlations display very different features. The classical correlations have initial rise and saturate at classical plateau, which indicate the environment has recorded redundant copies of system's classical information for independent observers. In sharp contrast, the quantum correlations raise when the nearly whole environment is accessed, manifesting quantum correlations cannot be shared between the observers [25]. Fig. 4b and c also demonstrate the effects of low-fidelity environment fragments (photons 5 and 6 in process $\vec{\theta}_B$), which will lead to early raise of quantum correlation (Fig. 4b) or delay the raise of classical correlation (Fig. 4c).

4. Discussion and conclusions

Our results exhibit that environment not only decoheres quantum system but also selectively delivers the system's information

to observers. The environment channel is high-efficient for classical information and inefficient for quantum information. Only the classical information of quantum system's decohered pointer states survives the environment-selected broadcasting and proliferates throughout the environment. Consequently, these results show that Quantum Darwinism theory predictions are compatible with the observation that classical objectivity originates from Darwinism-like broadcast structure of quantum substrate and quantum objectivity is prohibited by quantum mechanics due to quantum no-broadcast phenomenon [25,26].

In the experiment, the observation of quantum state is implemented by projection measurements with single photon counters, which is traditionally explained by wavefunction collapse from Copenhagen interpretation. The quantum Darwinism experiment provides a further detailed mechanism to the emergent classical objectivity during the observation of quantum state (the photon 1), in the case of multiple observers (the photons 2 to 6). This mechanism is not only compatible with the Copenhagen interpretation of quantum measurement but also demonstrates a concrete Everetts relative state [27,28] and thus consistent with the Many Worlds interpretation.

In summary, we have experimentally observed the classical objectivity emerging from classical information redundancy of single quantum system on a six-qubit quantum Darwinism simulator. We have demonstrated that the environment acting as communication channel and selectively broadcasting quantum system's pointer states are the crucial mechanism of quantum Darwinism. Our work presents an essential step to test the quantum Darwinism in small-scale controllable quantum environment. We expect further works to investigate the quantum Darwinism with more complex (e.g., larger-scale and mixed) quantum environment [17,20] along with the considerable progress of current experimental quantum simulation technology [11,29–31] and high-efficient quantum state characterization technology [32,33].
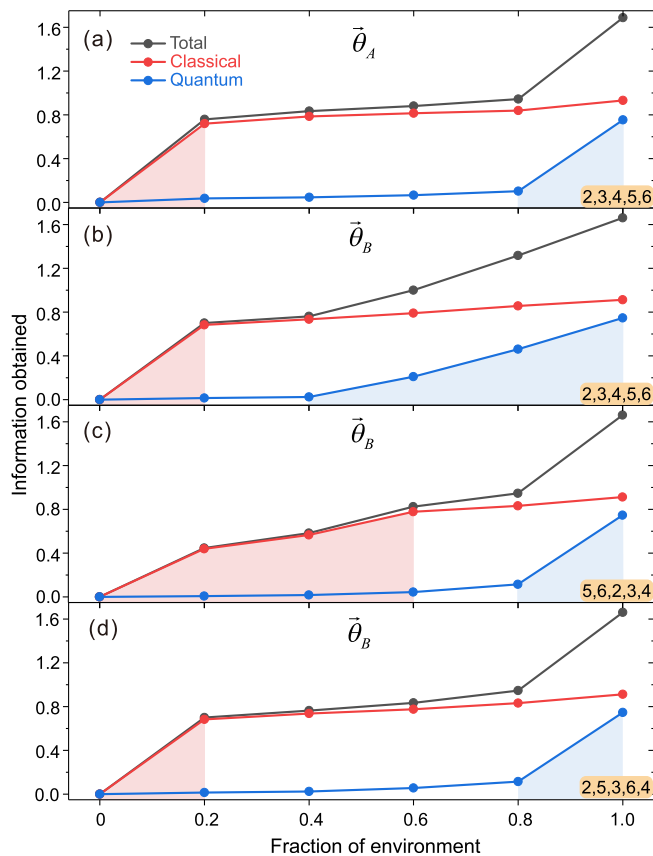
Fig. 4. (Color online) Accessible information of local observers. (a) Quantum Darwinism process $\vec{\theta}_A$. The total correlation, classical correlation (Holevo bound) and pure quantum correlation (quantum discord) between the system and the environment are shown. The fraction of environment increase in the order of photons 2, 3, 4, 5 and 6. (b), (c), (d) Quantum Darwinism process $\vec{\theta}_B$. The orders of environment photons are 23456, 56234 and 25364, respectively. One standard deviation is smaller than the size of data marker. Redundancy plateau of classical information correlation in environment fragments is observed meanwhile pure quantum correlation is suppressed due to the incompleteness of environment. Local observers use only small fraction of environment to infer the system, so only classical information is accessible.

Note

After completing our work, we became aware of two related experiments, one using two-photon four-qubit cluster state [34] and the other one using single NV center [35] to demonstrate quantum Darwinisim.

Conflict of interest

The authors declare that they have no conflict of interest.

Acknowledgments

Author contributions

M.-C.C., C.-Y.L., and J.-W.P. convinced and designed the work. M.-C.C., H.-S.Z., Y.L., D.W., X.-L.W., L.L., and N.-L.L. performed the experiment. M.-C.C., analyzed the data and wrote the manuscript with input from all authors. C.-Y.L. and J.-W.P. supervised the project.

Appendix A. Supplementary data

Supplementary data to this article can be found online at https://doi.org/10.1016/j.scib.2019.03.032.

References

[1] Schlosshauer M. Decoherence, the measurement problem, and interpretations of quantum mechanics. Rev Mod Phys 2005;76:1267.
[2] Bassi A, Lochan K, Satin S, et al. Models of wave-function collapse, underlying theories, and experimental tests. Rev Mod Phys 2013;85:471.
[3] Joos E, Zeh HD. The emergence of classical properties through interaction with the environment. Z Phys B Conden Matter 1985;59:223–43.
[4] Zurek WH. Decoherence, einselection, and the quantum origins of the classical. Rev Mod Phys 2003;75:715.
[5] Zurek WH. Quantum darwinism. Nat Phys 2009;5:181.
[6] Zurek WH. Quantum theory of the classical: quantum jumps, born's rule and objective classical reality via quantum darwinism. Phil Trans R Soc A 2018;376:20180107.
[7] Tuziemski J, Korbicz J. Analytical studies of spectrum broadcast structures in quantum brownian motion. J Phys A: Math Theor 2016;49:445301.
[8] Blume-Kohout R, Zurek WH. Quantum darwinism: entanglement, branches, and the emergent classicality of redundantly stored quantum information. Phys Rev A 2006;73:062310.
[9] Brandão FG, Piani M, Horodecki P. Generic emergence of classical features in quantum darwinism. Nat Commun 2015;6:7908.
[10] Lloyd S. Universal quantum simulators. Science 1996;273:1073–8.
[11] Aspuru-Guzik A, Walther P. Photonic quantum simulators. Nat Phys 2012;8:285.
[12] Vedral V. Classical correlations and entanglement in quantum measurements. Phys Rev Lett 2003;90:050401.
[13] Streltsov A, Kampermann H, Bruß D. Linking quantum discord to entanglement in a measurement. Phys Rev Lett 2011;106:160401.
[14] Modi K, Brodutch A, Cable H, et al. The classical-quantum boundary for correlations: discord and related measures. Rev Mod Phys 2012;84:1655.
[15] Zwolak M, Zurek WH. Complementarity of quantum discord and classically accessible information. Sci Rep 2013;3:1729.
[16] Riedel CJ, Zurek WH. Quantum darwinism in an everyday environment: Huge redundancy in scattered photons. Phys Rev Lett 2010;105:020404.
[17] Korbicz J, Horodecki P, Horodecki R. Objectivity in a noisy photonic environment through quantum state information broadcasting. Phys Rev Lett 2014;112:120402.
[18] Baumgratz T, Cramer M, Plenio M. Quantifying coherence. Phys Rev Lett 2014;113:140401.
[19] Streltsov A, Adesso G, Plenio MB. Colloquium: quantum coherence as a resource. Rev Mod Phys 2017;89:041003.
[20] Zwolak M, Quan H, Zurek WH. Redundant imprinting of information in nonideal environments: objective reality via a noisy channel. Phys Rev A 2010;81:062110.
[21] Kwiat PG, Mattle K, Weinfurter H, et al. New high-intensity source of polarization-entangled photon pairs. Phys Rev Lett 1995;75:4337.
[22] Pan J-W, Chen ZB, Lu CY, et al. Multiphoton entanglement and interferometry. Rev Mod Phys 2012;84:777.
[23] Einstein A, Podolsky B, Rosen N. Can quantum-mechanical description of physical reality be considered complete? Phys Rev 1935;47:777.
[24] Greenberger DM, Horne MA, Shimony A, et al. Bell's theorem without inequalities. Am J Phys 1990;58:1131–43.
[25] Streltsov A, Zurek WH. Quantum discord cannot be shared. Phys Rev Lett 2013;111:040401.
[26] Piani M, Horodecki P, Horodecki R. No-local-broadcasting theorem for multipartite quantum correlations. Phys Rev Lett 2008;100:090502.
[27] Everett III H. relative state formulation of quantum mechanics. Rev Mod Phys 1957;29:454.
[28] Wheeler JA. Assessment of everett's relative state formulation of quantum theory. Rev Mod Phys 1957;29:463.
[29] Houck AA, Türeci HE, Koch J. On-chip quantum simulation with superconducting circuits. Nat Phys 2012;8:292.
[30] Blatt R, Roos CF. Quantum simulations with trapped ions. Nat Phys 2012;8:277.

[31] Gross C, Bloch I. Quantum simulations with ultracold atoms in optical lattices. Science 2017;357:995–1001.
[32] Gross D, Liu Y-K, Flammia ST, et al. Quantum state tomography via compressed sensing. Phys Rev Lett 2010;105:150401.
[33] Torlai G, Mazzola G, Carrasquilla J, et al. Neural-network quantum state tomography. Nat Phys 2018;14:447.
[34] Ciampini MA, Pinna G, Mataloni P, et al. Experimental signature of quantum darwinism in photonic cluster states. Phys Rev A 2018;98:020101.
[35] Unden T, Louzon D, Zwolak M, et al. Revealing the emergence of classicality in nitrogen-vacancy centers. arXiv:1809.10456, 2018.

Chao-Yang Lu is a professor of physics at the University of Science and Technology of China. His research covers solid-state quantum photonics and quantum computing.

Ming-Cheng Chen is a postdoctoral research fellow at the University of Science and Technology of China. His research focuses on fundamental quantum physics and quantum computing using single photons and superconducting quantum circuits.